

Probability Density of the Multipole Vectors for a Gaussian Cosmic Microwave Background

Mark R Dennis^{1*}, Kate Land^{2†}

¹*School of Mathematics, University of Southampton, Highfield, Southampton SO17 1BJ, UK*

²*Oxford Astrophysics, Physics, DWB, Keble Road, Oxford, OX1 3RH, UK*

Accepted xxx. Received xxx; in original form xxx

ABSTRACT

We review Maxwell’s multipole vectors, and elucidate some of their mathematical properties, with emphasis on the application of this tool to the cosmic microwave background (CMB). In particular, for a completely random function on the sphere (corresponding to the statistically isotropic Gaussian model of the CMB), we derive the full probability density function of the multipole vectors. This function is used to analyze the internal configurations of the third-year Wilkinson Microwave Anisotropy Probe quadrupole and octopole, and we show the observations are consistent with the Gaussian prediction. A particular aspect is the planarity of the octopole, which we find not to be anomalous.

Key words: cosmic microwave background, spherical harmonics, Gaussianity

1 INTRODUCTION

The cosmic microwave background (CMB) is a unique cosmological probe. It is a window onto the early Universe, a backlight on the more recent, and it defines our observable Universe. It is therefore our best tool for investigating predictions of inflation theories, and cosmological scale properties of space, such as statistical isotropy. Predictions from inflation, such as homogeneity, isotropy, and the existence of Gaussian fluctuations, currently form the basis for our fundamental framework, with consequences for all other cosmological studies. It is therefore essential that we test these predictions, with appropriate tools. Current and future observations of the cosmic microwave background (CMB) provide us with a wealth of cosmological information, but they also confront us with many challenges. The large data-sets require novel data analysis and map-making techniques if we are to thoroughly exploit the data of its scientific information.

Since its launch in 2001, NASA’s Wilkinson Microwave Anisotropy Probe (WMAP) has observed the CMB over the full-sky, in five frequency bands between 22 and 90 GHz. Multiple frequency coverage has enabled reliable separation of the Galactic foreground signal from the CMB anisotropy, producing spectacular results (Spergel et al. 2003, 2006). The observations provide further support for the Λ CDM concordance cosmological model, and are remarkably consistent with a range of independent observations such as

the clustering of large-scale structure, and luminosity distances from Supernovae observations. However, some interesting features have been reported, on large-scales, which are anomalous with respect to our standard cosmological framework of a Gaussian statistically isotropic CMB. If an alternative framework is required, then this has far reaching consequences for the interpretation of all cosmological observations, and for the determination of cosmological parameter constraints (Hansen et al. 2004a).

On multipole scales $\ell \lesssim 60$ there is an asymmetrical distribution of power on the CMB sky, with more power in the southern ecliptic hemisphere (Eriksen et al. 2007, 2004a; Hansen et al. 2004b; Donoghue & Donoghue 2005). Similar asymmetrical signals have been seen with the bispectrum, n -point correlation functions, spherical wavelets, Minkowski functionals, genus statistic, and local curvature (Land & Magueijo 2005b; Eriksen et al. 2005; Vielva et al. 2004; Eriksen et al. 2004b; Park 2004; Hansen et al. 2004c).

A separate ‘anomaly’ involves just the largest scales, with $\ell = 2, 3$ correlated with each other and with the dipole direction (Copi et al. 2004, 2006; Ralston & Jain 2004; de Oliveira-Costa et al. 2004; Copi et al. 2007). Furthermore, $\ell = 4, 5$ are *also* seen to align with this ‘Axis of Evil’ direction (Land & Magueijo 2005a). Independently, $\ell = 3$ are reported to be particularly planar (Tegmark et al. 2003; de Oliveira-Costa et al. 2004; Schwarz et al. 2004), and the power on these scales is marginally low (Efstathiou 2004). The multipole vectors, described below, are an important tool in these studies.

However, the interpretation of these results is unclear.

* E-mail: mark.dennis@physics.org

† E-mail: krl@astro.ox.ac.uk

Different methods are employed, and various statistical measures invented, without systematically examining underlying mathematical properties of the representation. It is also not clear if some ‘anomalies’ are connected and thus over-reported, and a more systematic basis for tests of non-Gaussianity of the CMB is required. The usual harmonic n -point correlation functions, the bispectrum, trispectrum, etc., are unattractive as they are computationally intensive, abstract with relation to the underlying properties of the map, mutually dependent, contain redundant information, and are only meaningful under the assumption of statistical isotropy.

In this paper we revisit the multipole vectors, and study their mutual probability distribution for Gaussian maps. As an example of the general results, we consider the planarity of the octopole, but not the possibility of correlations in direction between different multipoles. The multipole vectors are a geometric representation of the spherical CMB map which is explicitly rotationally invariant, and whose probability distributions can be calculated for various Gaussian and non-Gaussian distributions of the CMB. They were introduced into cosmology and numerically analyzed by Copi et al. (2004), and were subsequently studied by Land & Magueijo (2005d,c); Dennis (2004, 2005); Lachieze-Rey (2004); Katz & Weeks (2004); Weeks (2004), among others. More recent astrophysical applications of the multipole vectors include further analysis of the CMB data (Rakic & Schwarz 2007), characterizing the peculiar velocity field of supernovae (Haugboelle et al. 2006), and quantifying systematic effects of dipole straylight contamination (Gruppuso et al. 2007).

Most of the multipole vector CMB analysis has involved a comparison of various derived quantities with the equivalent values from numerical Monte Carlo simulations; here, we present an alternative approach, based on analytic evaluation of the multipole vector probability distributions for statistically isotropic Gaussian random maps. We compute the full probability density function for the total multipole vector configuration, and use this to predict analytically the statistics of the multipole vector configuration. In Section 2 we introduce the multipole vectors and describe their numerical evaluation using polynomial root-finding algorithms (through the Majorana polynomial formalism); in Section 3 we review their properties for Gaussian random maps, and present the analytic Gaussian multipole vector probability density (calculated in the Appendix). In Section 4, these general statistical results are compared to the recent WMAP data at the largest scales, namely the quadrupole and octopole. In particular, we will describe an analytically tractable measure of planarity for the octopole, and demonstrate the WMAP data is very close to the Gaussian prediction. We conclude with a discussion in Section 5.

2 THE MULTIPOLE VECTORS

It is natural to represent data on the direction sphere (such as the cosmic microwave background) through the Fourier expansion

$$f(\theta, \phi) = \sum_{\ell \geq 0} \sum_{m=-\ell}^{\ell} a_{\ell m} Y_{\ell m}(\theta, \phi), \quad (1)$$

for the complex spherical harmonic functions

$$Y_{\ell m}(\theta, \phi) \equiv \sqrt{\frac{2\ell+1}{4\pi} \frac{(\ell-m)!}{(\ell+m)!}} P_{\ell}^m(\cos \theta) e^{im\phi}, \quad (2)$$

where $m = -\ell, -\ell+1, \dots, -1, 0, 1, \dots, \ell-1, \ell$, and P_{ℓ}^m is an associated Legendre polynomial. $Y_{\ell m}(\theta, \phi) = Y_{\ell m}(\mathbf{n})$ is the angular portion of the general solution to Laplace’s equation in spherical polar coordinates, and ℓ corresponds to the total angular momentum quantum number, and corresponds to an angular size of $\theta \sim 180^{\circ}/\ell$. All information in the map is now contained in the spherical harmonic coefficients $a_{\ell m}$, with reality of f enforced by the condition

$$a_{\ell, -m} = (-1)^m a_{\ell m}^*. \quad (3)$$

The expansion (1) for a fixed ℓ (‘multipole’) has $2\ell+1$ real degrees of freedom.

Following the Copernican principle – that there should be no special observers in the Universe – statistical isotropy (SI) is a natural assumption to make about the Universe. Assuming SI for all observers further implies homogeneity, and thus it is common for us to adopt the most general homogeneous and isotropic framework in cosmology, namely the Friedmann-Robertson-Walker metric. However, alternative frameworks exist, such as the anisotropic Bianchi models or the inhomogeneous Lemaître-Tolman-Bondi models. Preferred directions would also exist if the Universe had a non-trivial topology, or contained large-scale magnetic fields. SI of the CMB map is equivalent to the property that no quantity depends on any particular frame of reference – the map is statistically invariant to global rotations. Deviation from SI in the CMB observations would imply exotic physics in the early Universe or, perhaps more realistically, residual contamination by anisotropic foregrounds (e.g. emissions by Galactic diffuse components) or by residual systematic effects.

Such statistical properties of the spherical map can easily be conferred to the $a_{\ell m}$ s. We assume that any cosmic probability distribution of the $a_{\ell m}$ s is ergodic, that is, spatial averaging is equivalent to ensemble averaging, and such averaging is denoted $\langle \bullet \rangle$. Therefore, the 2-point correlation function can be written in terms of the $a_{\ell m}$ coefficients,

$$\langle f(\mathbf{n}_1) f(\mathbf{n}_2) \rangle = \sum_{\ell_1, 2, m_1, 2} \langle a_{\ell_1 m_1} a_{\ell_2 m_2} \rangle Y_{\ell_1 m_1}(\mathbf{n}_1) Y_{\ell_2 m_2}(\mathbf{n}_2), \quad (4)$$

and the action of a rotation R on the spherical harmonics involves the Wigner \mathcal{D} -function (rotation matrix element)

$$R[Y_{\ell m}(\mathbf{n})] = \sum_{m'} \mathcal{D}_{m' m}^{\ell} Y_{\ell m'}(\mathbf{n}). \quad (5)$$

The orthogonality condition of the \mathcal{D} -function,

$$\sum_m (-1)^{m_2-m} \mathcal{D}_{m_1 m}^{\ell_1} \mathcal{D}_{-m_2 -m}^{\ell_1} = \delta_{m_1 m_2}, \quad (6)$$

implies that $\langle f(\mathbf{n}_1) f(\mathbf{n}_2) \rangle$ is rotationally invariant (i.e. statistically isotropic) if and only if

$$\langle a_{\ell_1 m_1} a_{\ell_2 m_2}^* \rangle = \delta_{\ell_1 \ell_2} \delta_{m_1 m_2} C_{\ell_1}, \quad (7)$$

where C_{ℓ} is the *angular power spectrum*.

The issue of Gaussianity is separate from SI, and if the CMB fluctuations are Gaussian, then all the information in the map is contained in the 2-point correlation function, or

equivalently in the angular power spectrum C_ℓ as defined in (7); higher order functions – which otherwise probe non-Gaussianity – depend only on the 2-point correlation function, or are zero. SI is a consequence of Gaussianity, but there are other, non-Gaussian, statistically isotropic ensembles; this will be discussed further in Section 3.

An alternative representation to (1) of a function on a sphere is via the *multipole vectors* (MVs). For a real multipole of order ℓ , represented

$$f_\ell(\theta, \phi) = \sum_{m=-\ell}^{\ell} a_{\ell m} Y_{\ell m}(\theta, \phi), \quad (8)$$

with coefficients satisfying (3) (i.e. $f_\ell(x, y, z)$ is an eigenfunction of the Laplacian on the unit sphere ($x^2 + y^2 + z^2 = 1$) with eigenvalue $-\ell(\ell + 1)$), there exist ℓ unit vectors $\mathbf{v}_1, \dots, \mathbf{v}_\ell$ such that

$$f_\ell(x, y, z) = AD_{\mathbf{v}_1} \dots D_{\mathbf{v}_\ell} \frac{1}{r}, \quad (9)$$

where $D_{\mathbf{v}_i} = \mathbf{v}_i \cdot \nabla$ is a directional derivative operator, $r = (x^2 + y^2 + z^2)^{1/2}$ and A is a real constant. A more useful form of the representation is given by Dennis (2004),

$$f_\ell(\mathbf{n}) = B(\mathbf{n} \cdot \mathbf{v}_1) \dots (\mathbf{n} \cdot \mathbf{v}_\ell) + r^2 T, \quad (10)$$

where B is another real constant, and T is a scalar, given by the contraction of a certain Cartesian tensor of rank $\ell - 2$ with unit vector \mathbf{n} , which is fully determined by the 2ℓ components of the \mathbf{v}_i and is completely traceless and symmetric (Zou & Zheng 2003). A graphical representation of the $\ell = 2, 3, 4$ components of the WMAP temperature data of the CMB, together with their multipole vectors, is shown in Figure 1.

A simple way of connecting the two multipole representations (8) and (10) is using stereographic projection of the direction sphere (as the Riemann sphere) into the complex plane; thus the point on the sphere with coordinates θ, ϕ is stereographically mapped to the complex number $e^{i\phi} \tan(\theta/2)$. The stereographic images of the multipole vectors appear as the roots of the Majorana polynomial (spin coherent state) (Dennis 2004) (also see Helling et al. (2006)),

$$p(\zeta) = \sum_{m=-\ell}^{\ell} a_{\ell m} \mu_{\ell m} \zeta^{m+\ell}, \quad (11)$$

where $\mu_{\ell m}$ is a numerical factor,

$$\mu_{\ell m} \equiv (-1)^m \sqrt{\frac{(2\ell)!}{(\ell - m)!(\ell + m)!}}. \quad (12)$$

Thus $p(\zeta)$ is the complex polynomial acquired by replacing, in the expression (8), $Y_{\ell m}$ with $\mu_{\ell m} \zeta^{\ell+m}$. By the fundamental theorem of algebra, $p(\zeta)$ can be factorized:

$$p(\zeta) = a_\ell \prod_{i=1}^{2\ell} (\zeta - \zeta_i) = a_\ell \prod_{i=1}^{\ell} (\zeta - \zeta_i)(\zeta + 1/\zeta_i^*). \quad (13)$$

The vectors corresponding to the roots ζ_i form antipodal pairs since $a_{\ell-m} = (-1)^m a_{\ell m}^*$, implying that if ζ_i is a root, so is its antipode on the Riemann sphere $-1/\zeta_i^*$ (Dennis 2004), and we label the roots such that $\zeta_{i+\ell} = -1/\zeta_i^*$, i.e. $\zeta_i, \zeta_{i+\ell}$ are antipodal. The roots can be written in terms of modulus and argument,

$$\zeta_i = \tan(\theta_i/2) \exp(i\phi_i), \quad (14)$$

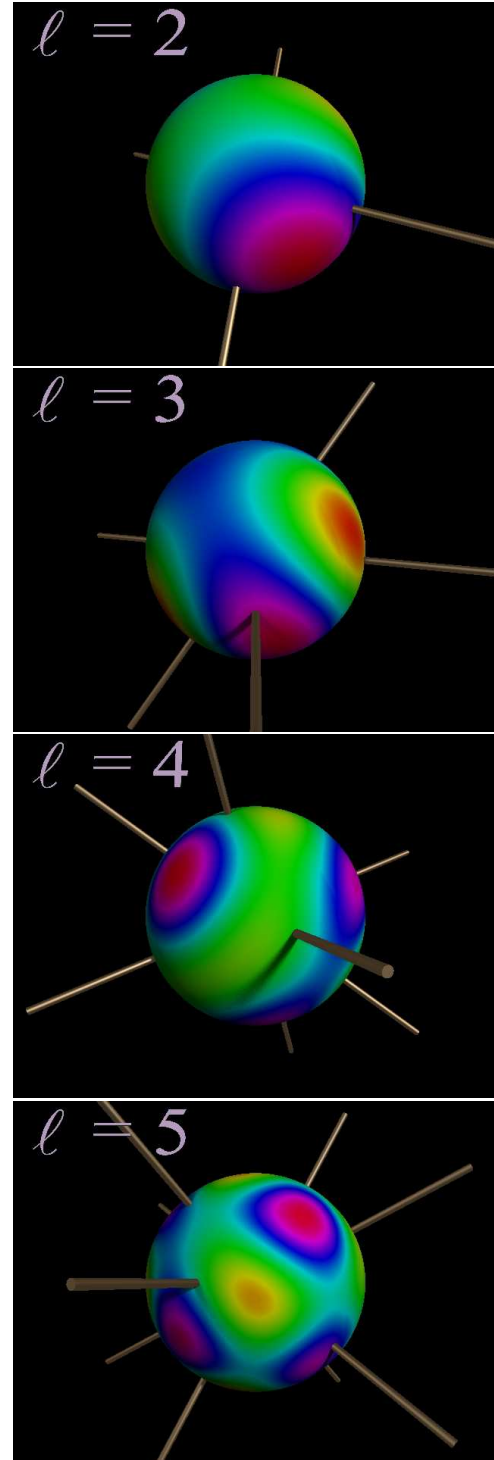


Figure 1. Representation of the multipole vectors for the WMAP3 multipoles $\ell = 2, 3, 4, 5$. The colour map on the spheres represents the underlying WMAP temperature data.

with θ_i, ϕ_i the spherical coordinates of the i th multipole vector.

The representations (11), (13) provide a simple method for computing the MVs, since the problem is reduced to finding the complex roots of a polynomial of order 2ℓ . Alternative methods include those of Copi et al. (2004) which use an iterative algorithm to solve (10), and a simi-

lar approach was previously outlined by Mezei & Campbell (1976), albeit in a different physical context. Obviously, all methods have limited numerical accuracy, due to the global nature of the problem. We note that numerical root-finding algorithms run into fundamental difficulties for high-order polynomials, due to problems of ill-conditioning and the limited numerical accuracy of the polynomial coefficients (i.e. the $a_{\ell m}$ coefficients); with 2 decimal place accuracy in the coefficients, practical root-finding is probably limited to $\ell \lesssim 20$ (Acton 1970). It is harder to locate the source of numerical error in the iterative approach. On account of these numerical problems, MVs have been studied in the CMB for lower multipoles, particularly for $\ell \leq 10$ (Copi et al. 2004; Land & Magueijo 2005d; Weeks 2004; Rakic & Schwarz 2007; Gruppiso et al. 2007; Haugboelle et al. 2006; Copi et al. 2006).

The MVs are, in fact, directors (‘headless vectors’), since their sign is globally undefined (a \pm transform on any pair of v_i leaves (9), (10) unchanged). Furthermore, just like roots of a polynomial, they are not ordered amongst themselves. Counting the degrees of freedom we see that for a multipole ℓ , there are 2ℓ degrees of freedom in the ℓ unit vectors, and one in the constant A in (9) (or B in (10)), agreeing with the $2\ell + 1$ freedoms in the $a_{\ell m}$ coefficients.

A simple example of the multipole vectors is those of a pure, real spherical harmonic $\text{Re } Y_{\ell m}$. Of the ℓ MVs, $\ell - |m|$ are aligned with the z -axis (in the $Y_{\ell m}$ frame) and the remaining $|m|$ vectors lie in the xy -plane, with vertices forming a regular $2m$ -polygon. Since this system of vectors rotates with the function, it is easy to identify pure harmonic modes in *any* frame of reference; the distribution of the $a_{\ell m}$ s of a pure mode in an arbitrary frame of reference is certainly not so transparent. This also applies to arbitrary multipoles, whose configuration of MVs rotates directly with rotation of the function, unlike the coefficients $a_{\ell m}$ (which change according to the appropriate \mathcal{D} -functions). This property makes the MVs an extremely useful tool for studying the statistical isotropy of the CMB - their configuration and statistics do not depend on the frame of reference. This avoids the problems inherent in manipulating the $a_{\ell m}$ s directly, and of having to find complicated rotationally invariant functions (bispectrum, trispectrum, etc.) which are hard to connect to underlying properties of the map and increasingly computationally intensive to compute. A drawback of the MVs is the problem of their numerical determination, described above.

The multipole vector formalism was apparently first introduced by Maxwell (Maxwell 1891), and is discussed in several classic mathematical textbooks (Hobson 1931; Courant & Hilbert 1953) (also see the references in Dennis (2004)). It has been applied in studies of quantum chemistry (Mezei & Campbell 1976) and continuum mechanics (Backus 1970; Zou & Zheng 2003). Its generalization to arbitrary spin states (where ℓ may be a half-integer and the coefficients $a_{\ell m}$ do not necessarily satisfy (3)) leads to the important canonical decomposition of totally symmetric spinors (Penrose & Rindler 1984) and the stellar representation of spin coherent states and $\text{SU}(2)$ polynomials (Bacry 1974; Bogomolny et al. 1996; Schupp 1999). In cosmology, the MV method has received considerable attention, from mathematicians exploring features of the formalism (Dennis 2005; Katz & Weeks 2004; Lachieze-Rey 2004; Weeks 2004;

Helling et al. 2006), and from astrophysicists applying it to the WMAP data of the CMB (Copi et al. 2006, 2004; Land & Magueijo 2005d).

In the following section, we will discuss the implications of different statistical assumptions of the $a_{\ell m}$ s on the probability distribution of the multipole vectors.

3 GAUSSIAN MODEL

A candidate ensemble for the $a_{\ell m}$ coefficients is ‘Gaussian’, that is, they are independent, identically distributed complex Gaussian random variables. Gaussianity of the CMB fluctuations is a generic prediction of simple inflation theories, because during slow-roll inflation the near flatness of the potential results in each Fourier mode of the inflaton perturbation evolving independently. This property translates to the density perturbations during reheating, and the central limit theorem implies their sum (i.e. into real space) will be Gaussian. Furthermore, the probability distribution for each Fourier mode is already expected to be Gaussian (if the perturbation is in the vacuum state). These models also predict that the Fourier modes have a near scale-invariant power spectrum. Even in these simple models, deviations from Gaussianity are expected on small scales where the central limit theorem breaks down. More complicated inflation models (Wands 2007; Rigopoulos et al. 2006), or alternative theories of structure formation such as topological defects (Battye 1999), can predict higher levels of non-Gaussianity.

Requiring SI alone is a far weaker assumption, that the probability density function (PDF) for the set of $a_{\ell m}$ s depends on rotationally invariant quantities (the angular power spectrum C_ℓ , bispectrum, trispectrum, etc.), and does not fix the ensemble uniquely. As described in the previous section, any probability density function (PDF) for the set of $a_{\ell m}$ coefficients satisfying (7) is statistically isotropic. For instance, it is possible to construct statistically isotropic ensembles which have a fixed MV configuration that is randomly oriented (for instance, for $\ell = 2$, the two MVs have the same – random – direction, equivalent to Y_{20} in some random frame). A Gaussian PDF, in which the $a_{\ell m}$ s are independent and Gaussian (with identical variance for same ℓ) clearly satisfies (7), and is unique in the property that its 2-point correlation function (or equivalently, its power spectrum) determines the ensemble uniquely; statistically isotropic non-Gaussian ensembles, whilst satisfying (7), have different n -point correlation functions (equivalently, averages of more than two $a_{\ell m}$ coefficients are non-Gaussian).

Nevertheless, there are other statistically isotropic PDFs which have the same MV distribution as the Gaussian model – using the MVs alone, it is impossible to distinguish Gaussianity uniquely from certain other ensembles. This wider class of ensembles is characterized by the property that the only quantity appearing in the PDF of the $a_{\ell m}$ s is $\hat{C}_\ell \equiv \sum_m |a_{\ell m}|^2 / (2\ell + 1)$; equivalently, the $(2\ell + 1)$ -dimensional vector $(a_{\ell, -\ell}, \dots, a_{\ell \ell})$ is invariant to all $(2\ell + 1)$ -dimensional unitary transformations preserving (3). In Dennis (2005), this wider class of ensembles was called *completely random*, as the statistics of the multipole f_ℓ depend only on the distribution of its normalization \hat{C}_ℓ , and the MVs have the same statistics for any completely

random ensemble, independent of the precise PDF of \hat{C}_ℓ . This may be understood from the polynomial representation (11): the MVs are distributed by the polynomial roots, whose distribution is independent of the any overall multiplicative factor of $p(\zeta)$, equivalent to \hat{C}_ℓ . Clearly, Gaussian distribution of the $a_{\ell m}$ s satisfies the condition to be completely random, and the PDF of \hat{C}_ℓ is that of the radius in a multidimensional isotropic Laplace distribution. A non-Gaussian example of a completely random ensemble is that in which \hat{C}_ℓ is absolutely fixed (its PDF is a δ -function); of course, such a distribution does not have any cosmological significance. Another completely random example is that of Gaussian and independent $a_{\ell m}$ s, apart from a cut forcing a maximum \hat{C}_ℓ . Such an ensemble was explored by Rakic & Schwarz (2007) – indeed, they observe that in this case the MVs are indistinguishable from the independent Gaussian case. If, in addition to complete randomness, the $a_{\ell m}$ s are also assumed independent (i.e. the full PDF factorizes, $P(\{a_{\ell m}\}) = P(a_{\ell,-\ell})\dots P(a_{\ell,\ell})$), then the completely random ensemble must be Gaussian (the argument is analogous to that of the Maxwell distribution in kinetic theory (Dennis 2005)). Another feature of all completely random ensembles – including the Gaussian – is that the PDFs for separate multipoles are completely independent. We will not examine this prediction against the CMB data in the present paper.

Perhaps counterintuitively, for a given ℓ , the MVs in the completely random case are *not* statistically independent, but have a unique joint probability distribution, which we derive exactly below. The derivation uses the fact that the MV distribution is equivalent to the probability distribution of the roots of the random Majorana polynomial (11), and is a special case of more general investigations of random polynomials (e.g. Hannay 1996; Bogomolny et al. 1996; Prosen 1996), where independent Gaussian random coefficients are assumed, although not the condition (3). In our analysis in Section 4, we will compare the MV distributions of the completely random model (including the Gaussian model) with that of independent MVs; although this latter does not have any obvious cosmological application, it is a non-Gaussian ensemble satisfying SI whose statistics are very simple to calculate analytically.

It has been previously shown (Dennis 2005; Land & Magueijo 2005c) that the 2-point function of the MVs exhibits quadratic repulsion (as usual for the roots of random polynomials and matrices (Bogomolny et al. 1996)). Given this repulsion, one may expect that the most probable MV distribution for fixed ℓ is at the vertices of the regular polyhedron with 2ℓ vertices, if it exists. If it does not exist, then there will be no unique maximal probability distribution (similar constructions for polynomials on the Riemann sphere are considered by Atiyah & Sutcliffe (2002)).

For any completely random distribution of the $a_{\ell m}$ coefficients, including the Gaussian distribution, the probability distribution for the ℓ multipole vectors $\mathbf{v}_1, \dots, \mathbf{v}_\ell$ can be found analytically, based on a transformation of the set of Gaussian-distributed coefficients $\{a_{\ell m}\}$ to the set of ℓ independent roots $\{\zeta_i\}$ of the Majorana polynomial (11). The full details of this calculation are given in the Appendix. For the multipole of order ℓ , the full joint probability density function of the ℓ multipole vectors $\{\mathbf{v}_i\}$, assuming dependence

only on \hat{C}_ℓ , is given by

$$P_\ell(\{\mathbf{v}_i\}) = \frac{(2\ell - 1)!! \prod_{j=1}^{2\ell} j!}{(2\pi)^\ell 2^{\ell^2} \ell!} \times \frac{\prod_{j,k=1, j < k}^{2\ell} \sin^2 \theta_{jk}}{\left(\sum_{\sigma \in S_{2\ell}} e^{i\alpha(\{\mathbf{v}_i\}, \sigma)/2} \prod_{j=1}^{2\ell} \cos \frac{\theta_{j, \sigma(j)}}{2} \right)^{\ell+1/2}}, \quad (15)$$

where θ_{jk} denotes the angle between the MVs labelled by j and k , and in the denominator, summation is over permutations σ in the set $S_{2\ell}$ of permutations on the 2ℓ indices $j = 1, \dots, 2\ell$; such a permutation gives rise to a system of piecewise-geodesic curves on the direction sphere (as each \mathbf{v}_j goes to $\mathbf{v}_{\sigma(j)}$ to $\mathbf{v}_{\sigma^2(j)}, \dots$), and $\alpha(\{\mathbf{v}_i\}, \sigma)$ is the signed solid angle on the sphere enclosed by these curves. It should be noted that $\mathbf{v}_{\ell+i} = -\mathbf{v}_i$, and the term in the denominator involves the 2ℓ -element set $\{\mathbf{v}_1, \dots, \mathbf{v}_{2\ell}\}$.

In practice, it is easier to work directly with the roots of the Majorana polynomial (stereographic images of the MVs in the complex plane), which have the probability distribution equivalent to (15),

$$P_\ell(\{\zeta_i\}) = \frac{(2\ell - 1)!! \prod_{j=1}^{2\ell} j!}{(2\pi)^\ell \ell! \prod_{j=1}^{2\ell} |\zeta_j|^2} \times \frac{\prod_{j,k=1, j < k}^{2\ell} |\zeta_j - \zeta_k|}{\left(\sum_{\sigma \in S_{2\ell}} \prod_{j=1}^{2\ell} (1 + \zeta_j \zeta_{\sigma(j)}^*) \right)^{\ell+1/2}}, \quad (16)$$

The function (15), and especially its stereographic counterpart (16), bears some similarity to the full probability distributions of roots of other Gaussian random polynomials representing spin states (Bogomolny et al. 1996; Hannay 1996): the discriminant of the polynomial in the numerator is divided by a combinatorial factor which mixes the roots nontrivially.

The functions $P_\ell(\{\mathbf{v}_i\})$ and $P_\ell(\{\zeta_i\})$ contain all the statistical information of the directions of the MVs, and the functions for different ℓ are mutually independent; the function (15) is one of the main results of this paper. The expressions (15) and (16) are unwieldy for high ℓ , primarily because the sum in the denominator involves $(2\ell)!$ terms, most of which are nontrivial.

In Dennis (2005), the 2-point multipole vector functions ρ_ℓ were calculated (corresponding to $P_\ell(\{\zeta_i\})$ only when $\ell = 2$). Normalized with respect to angle θ (between 0 and $\pi/2$), this is

$$\rho_\ell(\theta) = \sin \theta \left(\ell(\ell - 1)(1 + \cos \theta)^2 D^{5/2} \right)^{-1} \times \left\{ (2\ell D - 4buv - (b^2 + v^2)(a - 1 - u^2)) \times (dD - 2cuv(a + 1 - u^2) - (c^2 + av^2)(a - 1 - u^2)) + (2\ell D - 2cuv - buv(a + 1 - u^2) - v^2(a - 1 + u^2) - bc(a - 1 - u^2))^2 + (wD - 2bcu - uv^2(a + 1 - u^2) - bv(a - 1 + u^2) - cv(a - 1 - u^2))^2 \right\}, \quad (17)$$

with $D = (a - 1 - u^2 - 2u)(a - 1 - u^2 + 2u)$ and

$$\begin{aligned} a &= \sec^{4\ell} \frac{\theta}{2}, \quad b = 2\ell \tan \frac{\theta}{2}, \quad c = \ell \sin \theta \sec^{4\ell} \frac{\theta}{2}, \\ d &= 2\ell \sec^{4\ell-2} \frac{\theta}{2} \left(1 + 2\ell \tan \frac{\theta}{2} \right), \quad u = \tan^{2\ell} \frac{\theta}{2}, \\ v &= -2\ell \tan^{2\ell-1} \frac{\theta}{2}, \quad w = -2\ell(2\ell - 1) \tan^{2\ell-2} \frac{\theta}{2}. \end{aligned} \quad (18)$$

For the remainder of the paper, we will compare the full joint probability P_ℓ and the 2-point ρ_ℓ for the lowest two

nontrivial ℓ -components of the CMB distribution, namely the quadrupole $\ell = 2$, and octopole $\ell = 3$. This probability is shared by the Gaussian and other completely random ensembles; we will also compare the results for the ensemble of independent MVs. We will not be concerned here with issues of data analysis and error in determining the multipole vectors, but merely note that the full PDF enables the error in the multipole vector directions to be mapped directly to those in the $a_{\ell m}$ s. The $\ell = 2$ case was considered before (Land & Magueijo 2005c; Dennis 2005), but is included here for completeness; the $\ell = 3$ analysis is new.

4 COMPARISON WITH CMB DATA, $\ell = 2, 3$

For tests of statistical isotropy it is essential that we use full-sky maps, as a mask induces a relatively large anisotropic signal of its own. We therefore examine the ‘internal-linear-combination’ (ILC) maps of the WMAP collaboration. The WMAP mission (Spergel et al. 2003) produced full sky CMB maps from ten differencing assemblies (DAs). They also produced an ILC map, from combining smoothed frequency maps with weights chosen to minimize the rms fluctuations, using separate sets of weights for 12 disjoint sky regions. In the first-year data release the WMAP collaboration advised that the ILC map be used only as a visual tool. However, for the third-year release a thorough error analysis of the ILC map was performed, and a bias correction implemented (Hinshaw et al. 2006). The resulting third-year ILC map (herein WMAP3) is expected to be clean enough on scales $\ell \lesssim 10$ to be used without a mask¹.

As a consistency check we compare the WMAP3 data with some third-party maps, in which different methods of removing the foreground signal were employed. The third-year ILC map of Tegmark et al. (2003) (TOH herein), calculated using an ‘internal’ method (as WMAP), but with weights depending on scale in harmonic space as well as Galactic latitude. This is advantageous since different sources of contamination dominate at different scales - foregrounds at large scales, and noise at smaller scales. We also examine the map of Park, Park, & Gott (2007) (PARK herein), who employed an ILC method but fitting different weights over hundreds of disjoint regions rather than just 12. The final dataset is that produced by Bielewicz et al. (2005), who reconstructed the low-multipoles from high-latitude WMAP data by means of the power equalization filter method. We use their V-band map (PE herein).

For $\ell = 2$, in the Galactic frame, the multipole vectors of the WMAP3 are

$$\begin{pmatrix} -0.562 \\ 0.815 \\ 0.138 \end{pmatrix}, \begin{pmatrix} 0.971 \\ 0.048 \\ 0.234 \end{pmatrix}. \quad (19)$$

The angle between the quadrupole CMB vectors is 61.7° (to 1 decimal place). The resulting vectors are very similar for our third-party maps, although the inter-angle varies somewhat: {TOH, PARK, PE} = { 82.8° , 74.5° , 53.1° }. Due to the low number of degrees of freedom, the low- ℓ multipoles are particularly sensitive to the various treatments of the galactic plane (Naselsky, Verkhodanov, & Nielsen 2007).

However, as we will see, this variation does not effect our conclusions. Choosing the MVs (rather than their antipodes) such that the z -component of the MV is positive, the $\ell = 3$ WMAP3 vectors are

$$\begin{pmatrix} 0.905 \\ 0.401 \\ 0.145 \end{pmatrix}, \begin{pmatrix} 0.677 \\ -0.708 \\ 0.202 \end{pmatrix}, \begin{pmatrix} -0.051 \\ 0.770 \\ 0.636 \end{pmatrix}. \quad (20)$$

We label these $\mathbf{u}_0, \mathbf{u}_1, \mathbf{u}_2$ in sequence, and write down the three cosines between these vectors (which define the configuration uniquely)

$$\mathbf{u}_0 \cdot \mathbf{u}_1 = 0.358, \mathbf{u}_1 \cdot \mathbf{u}_2 = -0.451, \mathbf{u}_2 \cdot \mathbf{u}_0 = 0.353, \quad (21)$$

corresponding to angles between the directors of $69.0^\circ, 63.2^\circ, 69.3^\circ$ respectively. The MV director angles for the third-party maps are

$$\begin{aligned} \text{TOH} &: 68.9^\circ, 66.9^\circ, 73.8^\circ \\ \text{PARK} &: 65.4^\circ, 64.4^\circ, 73.5^\circ \\ \text{PE} &: 64.5^\circ, 62.1^\circ, 65.4^\circ. \end{aligned} \quad (22)$$

We now analyze these MVs with the Gaussian predicted statistics of Section 3. In subsection 4.1, we will discuss the 2-point MV correlation function and its comparison with the Gaussian 2-point function (17); in subsection 4.2, we will discuss how the octopole data compares with $P_3(\{\mathbf{v}_i\})$, and in subsection 4.3, we will discuss a natural measure of non-planarity for the octopole whose distribution can be almost-analytically handled by the Gaussian MV distribution function P_3 .

4.1 2-point multipole vector correlation functions

The 2-point correlation function probabilities were previously calculated in Dennis (2005), and studied numerically in Land & Magueijo (2005c). When $\ell = 2$, this is

$$\rho_2(\cos \theta) = \frac{27(1 - \cos^2 \theta)}{(3 + \cos^2 \theta)^{5/2}}. \quad (23)$$

Since the angle θ between the two multipole axes is the only degree of freedom for the $\ell = 2$ configuration, this is also the joint PDF $P_2(\{\mathbf{v}_1, \mathbf{v}_2\})$ of the multipole vectors for the quadrupole, and can be explicitly shown from (15). Normalizing over $0 \leq \theta \leq \pi/2$, therefore, we have

$$P_2(\theta) = \frac{27 \sin^3 \theta}{(3 + \cos^2 \theta)^{5/2}}. \quad (24)$$

In Fig. 2a, P_2 is plotted together with the WMAP3 data θ_{WMAP3} of 61.7° . The most preferred angle is 90° , with a probability of $\text{Prob}(\theta > 80^\circ) = 0.29$, and a median of $\theta \approx 72.2^\circ$. For the WMAP3 data we find $\text{Prob}(\theta < 61.7^\circ) = 0.28$, giving no indication of any significant discord between the data and the Gaussian (completely random) prediction. Similarly, the results from the third-party maps give are not significant as the lowest angle (for PE) finds $\text{Prob}(\theta < 53.1^\circ) = 0.16$. Thus there appears to be nothing anomalous about the distribution of the multipole vectors for $\ell = 2$.

When $\ell = 3$, the 2-point function is, from (17),

$$\rho_3(X) = \frac{75\sqrt{3}(1 - X^2)(3 + X^2)^2(88 + 67X^2 + 34X^4 + 3X^6)}{((4 - X + X^2)(4 + X + X^2)(5 + 3X^2))^{5/2}} \quad (25)$$

with $X = \cos \theta$. As with P_2 , the maximum occurs when

¹ WMAP data available from <http://lambda.gsfc.nasa.gov>

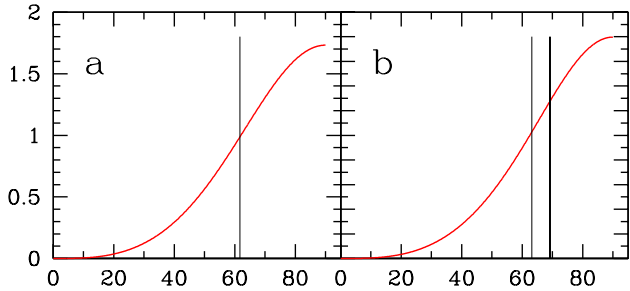


Figure 2. The 2-point correlation functions for Gaussian random multipoles, and the CMB WMAP3 data. a) $\ell = 2$, with angular separations $\theta_{\text{WMAP3}} = 61.7^\circ$; b) $\ell = 3$, with $\theta_{\text{WMAP3}} = 63.2^\circ, 69.0^\circ, 69.3^\circ$.

$\theta = 90^\circ$ – when the vectors are orthogonal. The function is plotted in Fig. 2b, together with the data from (21). We find, for the CMB data values, $\text{Prob}(\theta < \theta_3) = 0.29, 0.41, 0.42$ for $\theta_3 = 63.2, 69.0, 69.3^\circ$ respectively, with very similar results for the third-party maps. Thus, again the 2-point MV correlation function does not highlight anything anomalous about the octopole, although we look to the full joint PDF considered in the next subsection for a more complete analysis.

4.2 Full octopole Gaussian PDF

Since the PDF of any statistically isotropic ensemble is invariant to the choice of reference frame for the MVs, it is convenient to rotate the system of MVs $\mathbf{v}_0, \mathbf{v}_1, \mathbf{v}_2$ so that \mathbf{v}_0 points in the $+z$ -direction and \mathbf{v}_1 lies in the x, z -plane

There are therefore three parameters which govern the internal geometry of the system: the z -coordinate c_1 of \mathbf{v}_1 (i.e. $c_1 = \cos \theta_1$), the z -coordinate c_2 of \mathbf{v}_2 (i.e. $c_2 = \cos \theta_2$) and the relative azimuthal angle ϕ between \mathbf{v}_1 and \mathbf{v}_2 . Our chosen standard coordinate system is therefore

$$\mathbf{v}_0 = \begin{pmatrix} 0 \\ 0 \\ 1 \end{pmatrix}, \mathbf{v}_1 = \begin{pmatrix} s_1 \\ 0 \\ c_1 \end{pmatrix}, \mathbf{v}_2 = \begin{pmatrix} s_2 \cos \phi \\ s_2 \sin \phi \\ c_2 \end{pmatrix}, \quad (26)$$

where $s_j = \sin \theta_j = \sqrt{1 - c_j^2}, j = 1, 2$. However, due to the antipodal nature of the MVs, it is not appropriate to define c_1, c_2 over the whole sphere, and according to the labelling convention of (20), $c_1, c_2 \geq 0$ (i.e. the MV axis is labelled by the vector in the northern hemisphere).

Using (21), it is straightforward to determine that, for the CMB MV data (20) (with the same ordering),

$$\begin{aligned} c_{1,\text{WMAP3}} &= \mathbf{u}_0 \cdot \mathbf{u}_1 = 0.358, \\ c_{2,\text{WMAP3}} &= \mathbf{u}_0 \cdot \mathbf{u}_2 = 0.353, \\ \phi_{\text{WMAP3}} &= \arg(\mathbf{u}_0 \times \mathbf{u}_1) \cdot (\mathbf{u}_0 \times \mathbf{u}_2 + i\mathbf{u}_2) = -2.293. \end{aligned} \quad (27)$$

These are readily checked by verifying that the scalar products of (26) agree with (21), and that the scalar triple product is the same for the two sets of vectors.

The full $\ell = 3$ octopole PDF P_3 is given by (15) (actually, computed using (16)), is significantly simplified by choosing the MVs in the standard coordinate system (26),

reducing to

$$P_3(c_1, c_2, \phi) = \frac{750\sqrt{3}s_1^2s_2^2(1 - (c_1c_2 + s_1s_2 \cos \phi)^2)}{\pi(5 + 3c_1^2 + 3c_2^2 + (c_1c_2 + s_1s_2 \cos \phi)(c_1c_2 + 3s_1s_2 \cos \phi))^{7/2}}. \quad (28)$$

It is evident that c_1 and c_2 appear on an equal footing, as they should. Further, because the multipole vectors are not naturally ordered, this PDF does not depend on their ordering (although the exact equation for parameter ϕ in (27) depends on the xy -quadrant \mathbf{u}_2 occupies in the rotated standard coordinate system).

P_3 is normalized, i.e.

$$\int_0^1 dc_1 \int_0^1 dc_2 \int_0^{2\pi} d\phi P_3(c_1, c_2, \phi) = 1, \quad (29)$$

which is easily checked numerically. Our choice of parameters is such that the probability density element $dc_1 dc_2 d\phi$ is uniform. In the model in which the MVs are statistically isotropic and completely independent, the PDF for c_1, c_2, ϕ (over the same integration domain) would evidently be constant $1/2\pi$.

The 3-dimensional distribution of $P_3(c_1, c_2, \phi)$ is shown in Fig. 3. It is clear from the figure that the maximally probable distribution of the MV axes is mutually perpendicular, that is $c_1 = c_2 = 0, \phi = \pm\pi/2$, or $|\mathbf{v}_0 \cdot (\mathbf{v}_1 \times \mathbf{v}_2)| = 1$. This supports the previous statement that the unique maximal probability configuration exists when 2ℓ is the number of vertices of a regular polyhedron, in this case an octahedron (whose six vertices are mutually perpendicular), and the MV configuration falls into the octahedral symmetry group (the octopole function with maximum probability ($\propto xyz \propto iY_3^2 - iY_3^{-2}$) has tetrahedral symmetry, not being inversion-symmetric).

This maximal probability occurs with probability density $6\sqrt{3}/\sqrt{5}\pi \approx 1.48$, about 9 times that for independent MVs. The probability is low when the MVs are nearby, demonstrating repulsion as with the 2-point MV function.

The MV directions of the octopole CMB data are represented in Fig. 4, and this has probability density 0.362, which can be compared to the maximum (orthogonal configuration) with a probability density of 1.479, and the minimum (all aligned) with zero. We find that 87.4% of the $\{c_1, c_2, \phi\}$ configuration space has a probability density less than 0.362, and thus the WMAP3 octopole MV configuration is not improbable. The third-party maps (TOH, PARK, PE) have octopole configurations with probability densities 0.484, 0.380, 0.252 respectively (with 91.5%, 88.2%, 81.2% of configuration space with lower probability density). Thus, according to the Gaussian multipole vector joint probability density function, there is nothing particularly anomalous about the $\ell = 3$ configuration of the multipole vectors, in agreement with Land & Magueijo (2005a, 2006).

This contrasts with the findings of Tegmark et al. (2003); de Oliveira-Costa et al. (2004); Schwarz et al. (2004), in which the octopole data is interpreted to be remarkably planar. That is to say, the multipole vectors tend to lie equally spaced in a plane, or equivalently the octopole is dominated by $Y_{3,3}$ in some frame. These claims were re-examined in Copi et al. (2006), where planarity was found with a reduced evidence of only 89% Confidence Limit, using the same statistic. Indeed the vectors do tend to lie in a plane, but this does not appear to be

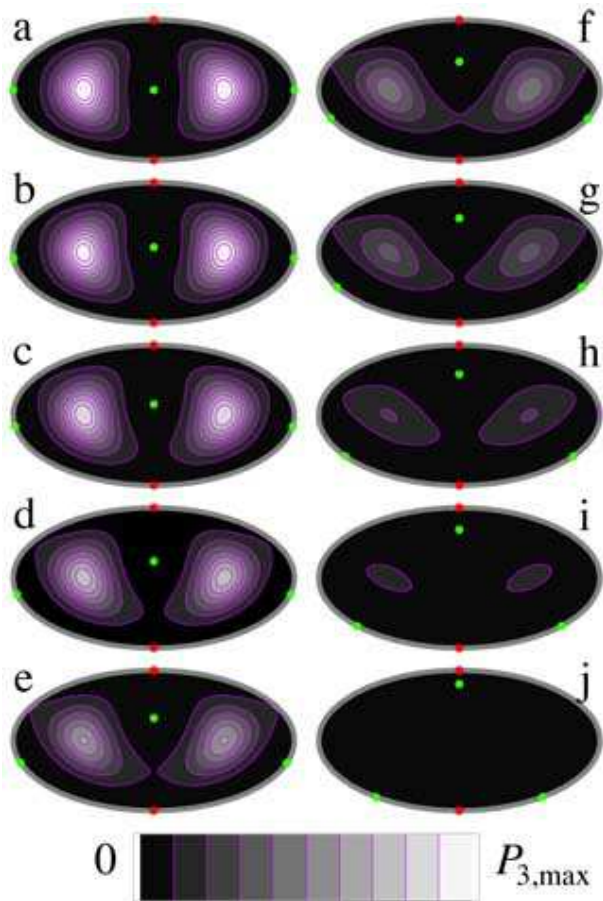


Figure 3. A representation of the 3-dimensional octopole vector PDF $P_3(c_1, c_2, \phi)$ from (28), in standard configuration. Each frame a-j represents a different position of $c_1 < 1$ (the green dot on the vertical axis), and is a plot over the θ_2, ϕ -sphere in Mollweide projection. Frame a has $c_1 = 0$, increasing in increments of 0.1 to frame j, with $c_1 = 0.9$ (since $P_3(1, c_2, \phi) = 0$). The fixed MV axis in $\pm \hat{z}$ is represented by red dots at the north and south poles, and the opposite vector to \mathbf{v}_1 is shown on each side of the plot (at $\phi = \pm\pi$) as green dots. For each frame (with fixed c_1), the shading represents the probability $P_3(c_1, c_2, \phi)$, that is, the position of the MV $\pm \mathbf{v}_2$ (parameterized by θ_2, ϕ). Contours are plotted at values of $P_{3,\max}/10$. If the probability density function were uniform over c_1, c_2, ϕ , the uniform density would be about the level of the lowest contour line.

particularly anomalous. The reason for the disagreement originates in the particular statistical measure used, and various measures have been introduced in the literature, based upon their ease for numerical computation. Here, we develop an alternative, analytic approach based on the full joint probability distribution of the multipole vectors, which complements the other numerical approaches. As can be seen from Fig. 4, the multipole vectors can have a significantly planar configuration while not being anomalous with respect to a Gaussian distribution. In the following subsection, we study octopole planarity further by calculating the statistics for a natural measure of MV planarity. It should be noted that the discussions of the papers cited above, significance is added to the observed planarity of the octopole by its correlation with the orien-

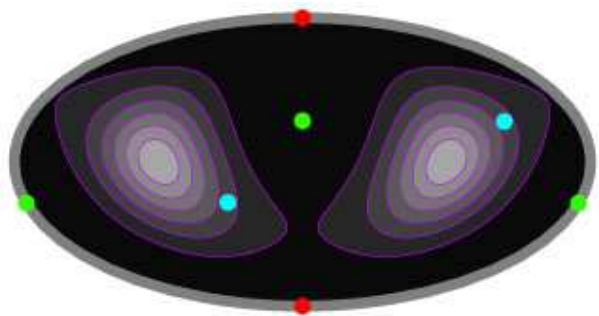


Figure 4. A representation, in the style of Fig. 3, showing the CMB WMAP3 octopole, with the θ_2, ϕ distribution with $c_1 = 0.358$ fixed. The third WMAP3 multipole vector with coordinates $(\phi, c_2) = (48.6^\circ, 0.353)$ and its antipode are represented as a light blue pair of dots. The scale of the plot is the same as in Fig. 3.

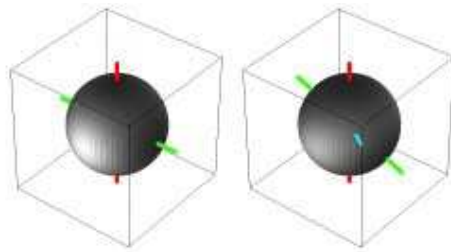


Figure 5. A further representation of Figs. 3a and 4, plotted now on the surface of the sphere. The multipole vector axes are represented by the same colours as before.

tation of the observed quadrupole; we make no comment on inter-multipole orientations here.

Comparing with the ensemble of the completely independent MVs model, whose probability density is constant $1/2\pi \approx 0.159$ (about the lowest contour line level in Figs. 3, 4) the CMB data is obviously more likely to originate from a Gaussian distribution of $a_{\ell m}$ coefficients. The plots of Figs. 3a and 4 are plotted spherically in Fig. 5.

4.3 Statistics of planarity of $\ell = 3$ multipole vectors

Using the analytically-calculated probability density function for the three multipole vectors of the cosmic octopole, it is possible to predict exactly the non-planarity statistics of the Gaussian model.

As we described above, up to a global rotation, the octopole vectors have three degrees of freedom, and the full joint probability density function of these vectors is given for the Gaussian model in (28). We will compare this with the ensemble with completely independent MVs, whose joint PDF for c_1, c_2, ϕ is the constant $1/2\pi$.

An analytically natural measure of (non-)planarity of the multipole vectors $\mathbf{v}_0, \mathbf{v}_1, \mathbf{v}_2$, is the magnitude of the scalar triple product

$$\begin{aligned} \tau &\equiv |(\mathbf{v}_0 \times \mathbf{v}_1) \cdot \mathbf{v}_2| \\ &= |s_1 s_2 \sin \phi| \end{aligned} \quad (30)$$

for \mathbf{v}_i given by (26), where $s_i = \sqrt{1 - c_i^2}$. The sign of the

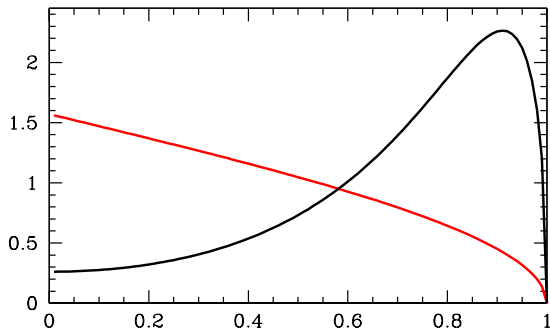


Figure 6. Plots of the probability density functions of the multipole vector non-planarity τ for the two ensembles: Gaussian model (black) and uncorrelated multipole vectors (red).

triple product has no meaning, as the ordering of the vectors is arbitrary, as is the choice of \pm direction of the \mathbf{v}_j . Geometrically, τ is the volume of the parallelepiped with edges $\mathbf{v}_0, \mathbf{v}_1, \mathbf{v}_2$. Clearly it is 0 if and only if the vectors are coplanar (linearly dependent), and it is 1 if and only if they are orthogonal. τ does not directly determine the spacing of the MVs; in the data, not only are the MVs nearly planar, they are also quite uniformly spaced (their angles are all $\approx 60^\circ$). Any planarity measure, including τ , depends on the pairwise spacing of the MVs as well as their overall planarity.

In other studies, the normalized angular momentum dispersion, maximized over all directions, is used as the measure of octopole planarity (de Oliveira-Costa et al. 2004; Copi et al. 2006). This quantity, which positively weights octopole configurations with equally spaced MVs ($a_{3,3} + a_{3,-3}$ in some frame), is rather hard to analyze using the analytical methods here; τ is used as an alternative planarity measure which is mathematically natural – (30) is the simplest quantity to combine three vectors in three dimensions – although equally spaced planar MVs, as opposed to any other planar configuration, are not particularly distinguished. τ is properly a measure of non-planarity (being smaller the more planar the configuration), and we henceforth adopt this description.

In the Appendix, the PDF of τ is derived for the Gaussian model and the independent MVs model. For the Gaussian model, the PDF is written down as a certain double integral which can be integrated numerically for each τ . In the independent MVs case, the PDF is simply

$$P_{\text{ind}}(\tau) = \arccos \tau. \quad (31)$$

Plots of the PDFs for τ for the two ensembles are presented in Fig. 6: the uncorrelated ensemble tends to have a lower (more planar) value of τ than the Gaussian model, on account of the repulsion of the MVs for the Gaussian ensemble. The first two moments in each case are

$$\begin{aligned} \langle \tau \rangle_{\text{ind}} &= \pi/8 \approx 0.393, \\ \langle \tau^2 \rangle_{\text{ind}} &= 2/9 \approx 0.222, \\ \langle \tau \rangle_{\text{Gauss}} &= 0.686, \\ \langle \tau^2 \rangle_{\text{Gauss}} &= 0.529. \end{aligned} \quad (32)$$

Thus, for the Gaussian model, although the configuration with maximum probability has orthogonal multipole vec-

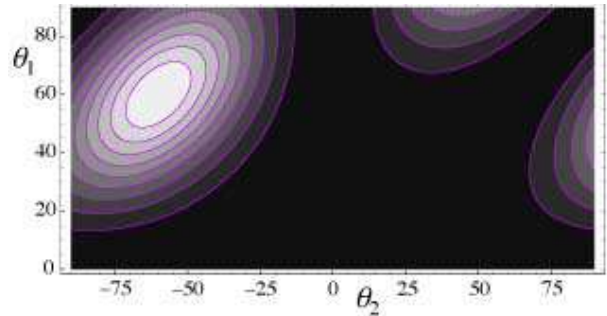


Figure 7. Probability distribution of the multipole vector configuration conditional on a planar arrangement. The vertical axis is θ_1 , the horizontal θ_2 , both in degrees (with $0 \leq \theta_1 \leq 90^\circ$, $-90^\circ \leq \theta_2 \leq 90^\circ$ for all possible planar configurations).

tors, corresponding to $\tau = 1$, the mean τ is less than 0.7. The data for WMAP3 map, with octopole multipole vectors given by (20), has a non-planarity measure of

$$\tau_{\text{WMAP}} = 0.655, \quad (33)$$

which is surprisingly high given the literature on the apparent anomalous planarity of the octopole; for the Gaussian model this value is in very good agreement with the mean. As described above, this difference arises in the choice of τ , rather than other measures, as planarity measure.

For the third-party maps, τ has values 0.749 (TOH), 0.676 (PARK) and 0.505 (PE).

The full probability density (28) may also be used to investigate the behaviour of the multipole vectors if they are constrained to be planar; in the present parameterization, this is equivalent to the restriction $\phi = 0$ (the possibility that $\phi = \pi$ has been replaced by an extended range for θ_2 , $-90^\circ \leq \theta_2 \leq 90^\circ$). With these restrictions, the probability distribution (for integration with respect to $dc_1 dc_2$) is proportional to

$$P_{\text{Gauss}}(\theta_1, \theta_2 | \text{planar}) = A \frac{\sin^2 \theta_1 \sin^2 \theta_2 \sin^2(\theta_1 - \theta_2)}{(9 + \cos 2\theta_1 + \cos 2\theta_2 + \cos 2(\theta_1 - \theta_2))^{7/2}}, \quad (34)$$

where A is a normalization constant. This distribution is plotted in Fig. 7. Although it is obvious that the most likely configuration with enforced planarity is with multipole vectors maximally distant (i.e. $\theta_1 = 60^\circ, \theta_2 = -60^\circ$), this distribution quantifies this precisely for the Gaussian model.

5 DISCUSSION

We have reviewed the multipole vector method of interpreting CMB maps, including an analytic computation of the full probability density function of the multipole vectors for the statistically isotropic Gaussian random model. We analyzed this function for $\ell = 2, 3$, and a comparison with data revealed that the third-year WMAP data is consistent with the Gaussian model, despite the apparent anomalous planarity of the octopole.

A natural extension of this work is to provide a full PDF analysis of the higher multipoles; however, this is

mathematically complicated. P_3 depends on three parameters, and therefore can be plotted (as in Fig. 3) as a 1-parameter family of 2-dimensional maps. The next multipole, $\ell = 4$, requires five parameters to specify the multipole vector configuration, and P_5 requires 7. In addition to this increase of parameters, the term in the denominator of the PDF (15), (16), summing over $(2\ell)!$ permutations of the MVs, becomes significantly more difficult to compute as ℓ increases. For $\ell > 20$ the problem is exacerbated by the limited numerical accuracy of the various MV-finding algorithms. It is clear that as we extend the work to higher multipoles, statistics based on derived quantities, rather than the full PDF, will be necessary. Furthermore, we have not addressed the important issue of inter- ℓ correlations (Land & Magueijo 2005a, 2006), or correlations between the CMB and external reference frames – as pointed out by Tegmark et al. (2003); de Oliveira-Costa et al. (2004); Schwarz et al. (2004); Copi et al. (2006, 2007), the apparent plane of the octopole is strongly aligned with the orientation of the dipole. Such correlations are indicative of a breakdown of SI, independent from any assumption about the distribution of the $a_{\ell m}$ s.

Thus, we defer to a future work a study where measures of anisotropy will be constructed from the MVs, in place of the full probability density function. These anisotropy measures must be defined to be as orthogonal as possible so to avoid a repetition of information. Also, the MVs will be used to systematically define a Cartesian frame for each multipole, so to probe the orientation and inter- ℓ correlations of the multipoles, and thus probe the issue of SI independently of any assumptions about Gaussianity.

It is fortuitous that the standard model for the CMB, namely Gaussian distributed $a_{\ell m}$ coefficients, corresponds precisely to the case studied for spin coherent SU(2) polynomials (Bogomolny et al. 1996; Hannay 1996), with the additional constraint (3). This means that quantities such as the 2-point MV correlation function ρ_2 , the full MV joint PDF P_ℓ , and, in fact, any N -point MV correlation function (Dennis 2005) can be calculated exactly analytically using the methods of random polynomials. This suggests the application to the CMB of other ideas from other fields this technique is used, such as random spins (Hannay 1996), Renyi-Werhl entropy (Helling et al. 2006), Skyrmion analysis (Atiyah & Sutcliffe 2002), and quantum chaos (Bogomolny et al. 1996), which may provide other powerful tools to analyze cosmological maps.

One of the most difficult aspects of CMB analysis is, of course, that we are provided with only one sample function to test our statistics: the observed Universe. This fact is all the more apparent at the low multipoles where there are only a small number of degrees of freedom. As it is precisely these few data points that probe the largest scales in the Universe, it is essential that we hone our statistics to exploit the low-multipoles of the CMB as carefully as possible.

ACKNOWLEDGEMENTS

We are grateful to John Hannay, Joao Magueijo, Glenn Starkman and James Vickers for discussions. KRL is funded by the Glasstone Research Fellowship and Christ Church

college, Oxford, MRD by a Royal Society University Research Fellowship.

APPENDIX

Derivation of the full MV PDF (15)

The coefficients of any polynomial can be written in terms of the roots, the so-called *symmetric polynomials*. In the present case,

$$p(\zeta) = a \exp\left(-i \sum_{i=1}^{\ell} \phi_i\right) \sum_{m=-\ell}^{\ell} (-1)^{\ell-m} s_{\ell-m} \zeta^{m+\ell}, \quad (35)$$

where s_n is the n th symmetric polynomial for the polynomial of order 2ℓ (with $2\ell + 1$ coefficients, $n = 0, \dots, 2\ell + 1$),

$$s_n = \sum_{1 \leq i_1 < i_2 < \dots < i_n \leq 2\ell} \prod_{k=1}^n \zeta_{i_k}, \quad (36)$$

and the factor $a \exp\left(-i \sum_{i=1}^{\ell} \phi_i\right)$ is the coefficient for $\zeta^{2\ell}$. Therefore

$$\mu_m a_{\ell m} = a \exp\left(-i \sum_{i=1}^{\ell} \phi_i\right) (-1)^{\ell-m} s_{\ell-m}. \quad (37)$$

a is a real number since the overall phase factor of a_ℓ is fixed. Since $s_0 = 1$, and $s_{2\ell} = \prod_{i=1}^{2\ell} \zeta_i = \exp\left(2i \sum_{i=1}^{\ell} \phi_i\right)$, then

$$a_{-\ell} = (-1)^\ell a \exp\left(-i \sum_{i=1}^{\ell} \phi_i\right) s_{2\ell} = (-1)^\ell a_\ell^*. \quad (38)$$

By hypothesis, the coefficients a_0, a_1, \dots, a_ℓ are independent and identically distributed Gaussians (a_0 is real, the others complex). The correctly normalized total probability distribution is therefore

$$\begin{aligned} P(\{a_{\ell m}\}) &= \frac{1}{\sqrt{2\pi}^{\ell+1/2}} \exp\left(-\frac{a_0^2}{2} - \sum_{m=1}^{\ell} |a_{\ell m}|^2\right) \\ &= \frac{1}{\sqrt{2\pi}^{\ell+1/2}} \exp\left(-\frac{1}{2} \sum_{m=-\ell}^{\ell} \frac{a^2 |s_{\ell+m}|^2}{\mu_m^2}\right) \\ &= \frac{1}{\sqrt{2\pi}^{\ell+1/2}} \exp\left(-\frac{1}{2} \frac{a^2}{2(2\ell)!} \Sigma\right). \end{aligned} \quad (39)$$

In the second line, $|a_{\ell m}|^2$ has been replaced with $(|a_{\ell m}|^2 + |a_{-\ell-m}^2|)/2 = a^2(|s_{\ell+m}|^2 + |s_{\ell-m}^2|)/2\mu_m^2$ using (37). In the final line, the quantity Σ has been introduced, where

$$\Sigma \equiv \sum_{i=0}^{2\ell} i!(2\ell-i)! |s_i|^2 = \sum_{\sigma \in S_{2\ell}} \prod_{i=1}^{2\ell} (1 + \zeta_i \zeta_{\sigma(i)}^*), \quad (40)$$

where the second equality, in which Σ is realized as a sum over permutations σ over the 2ℓ roots, was observed by Hannay (1996). The quantity $\hat{C}_\ell \equiv \sum_{m=-\ell}^{\ell} |a_{\ell m}|^2 / (2\ell + 1)$, described in Section 3, equals $a^2 \Sigma / 2(2\ell)!$ by (39). The PDF of any completely random ensemble depends only on this quantity.

In order to write the probability density (39) as a distribution over the multipole vector root configuration, it is necessary to find the appropriate Jacobian $\{a_{\ell m}\} \rightarrow \{\zeta_i\}$.

Using standard methods (e.g. Bogomolny et al. (1996)) it is straightforward to show that

$$d^{2\ell+1}\{a_{\ell m}\} = \frac{a^{2\ell}}{\prod_{m=-\ell}^{\ell} |\mu_m| \prod_{j=1}^{\ell} |\zeta_j|^2} \mathcal{D} da d^{2\ell}\{\zeta_j\}. \quad (41)$$

where \mathcal{D} is the square root modulus of the polynomial discriminant,

$$\mathcal{D} = \prod_{i,j=1, i < j}^{2\ell} |\zeta_i - \zeta_j|. \quad (42)$$

The final joint PDF for the multipole vectors is the integral of this quantity with respect to a ($-\infty < a < \infty$) (using the Gaussian probability density (39)). It must be divided through by $\ell!$ (since the ℓ independent roots are indistinguishable), and 2^ℓ (since $\zeta_j, \zeta_{j+\ell}$ are indistinguishable for $j = 1, \dots, \ell$):

$$\begin{aligned} P_\ell(\{\zeta_i\}) &= \frac{1}{\ell!(2\pi)^{\ell+1/2}} \frac{\mathcal{D}}{\prod_{m=-\ell}^{\ell} |\mu_m| \prod_{j=1}^{\ell} |\zeta_j|^2} \times \\ &\int da a^{2\ell} \exp\left(-\frac{a^2}{2(2\ell)!}\Sigma\right) \\ &= \frac{(\ell-1/2)!}{\ell!\pi^{\ell+1/2}} \frac{(2\ell)!^{\ell+1/2} \mathcal{D}}{\Sigma^{\ell+1/2} \prod_{m=-\ell}^{\ell} |\mu_m| \prod_{j=1}^{\ell} |\zeta_j|^2}. \end{aligned} \quad (43)$$

Rearranging the numerical prefactor, $(\ell-1/2)!/\pi^{\ell+1/2} = (2\ell-1)/(2\pi)^\ell$, and $(2\ell)!^{\ell+1/2}/\prod_{m=-\ell}^{\ell} |\mu_m| = \prod_{j=1}^{2\ell} j!$. Finally, substituting Σ via (40) gives (16).

In order to transform from the stereographic plane to the direction sphere, it is necessary to multiply by the stereographic Jacobian factor $2^{-\ell} \prod_{j=1}^{\ell} (1 + |\zeta_j|^2)^2$ (this factor differs from the usual stereographic Jacobian factor by 2^ℓ , since the labelling MVs are in the northern hemisphere, meaning that $|\zeta_j| \leq 1$ for $j = 1, \dots, \ell$). Substituting the roots by (14), with appropriate interpretation on the direction sphere (Hannay 1996) gives the joint probability density function (15).

Derivation of the τ PDF

The probability density function for τ is found by substitution of $\phi \rightarrow \tau$ by

$$\phi = \arcsin\left(\frac{\tau}{s_1 s_2}\right). \quad (44)$$

The Jacobian of this transformation is

$$\frac{d\phi}{d\tau} = \frac{1}{\sqrt{s_1^2 s_2^2 - \tau^2}} \quad (45)$$

The derivation of the PDF for τ in the independent MVs model is easy, as the PDF is constant with respect to the volume element $dc_1 dc_2 d\phi$. The PDF can therefore be calculated from the c_1, c_2, ϕ normalization integral, with ϕ substituted by τ using (44) and (45), then integrating c_1 and c_2 . This integral is

$$1 = \frac{2}{\pi} \int_0^1 dc_1 \int_0^1 dc \int_0^{\sqrt{(1-c_1^2)(1-c_2^2)}} d\tau \frac{1}{\sqrt{(1-c^2)(1-c_1^2) - \tau^2}}. \quad (46)$$

Without changing the integrand, the order of integration is changed to c_2 , then c_1 , then τ last, with $0 \leq c_2 \leq$

$\sqrt{1-\tau^2/(1-c_1^2)}$, $0 \leq c_1 \leq 1-\tau^2$, then $0 \leq \tau \leq 1$. Finally, c_1 and c_2 are rescaled in order that the volume of integration is again a cube:

$$1 = \frac{2}{\pi} \int_0^1 d\tau \int_0^1 dc_1 \int_0^1 dc_2 \frac{\sqrt{1-\tau^2}}{\sqrt{(1-c_1^2)\sqrt{(1-c_2^2(1-\tau^2))}}}. \quad (47)$$

c_1 and c_2 may now be integrated directly,

$$1 = \int_0^1 d\tau \arccos \tau, \quad (48)$$

giving the PDF of equation (31).

The strategy for the Gaussian model is identical, although the integrand in (46) is multiplied by the Gaussian model PDF (29), with ϕ substituted by τ . The final Gaussian τ PDF therefore can be written in terms of a double integral,

$$\begin{aligned} P_{\text{Gauss}}(\tau) &= \frac{1500\sqrt{3}\eta}{\pi} \int_0^1 dc_1 \int_{-1}^1 ds_2 \times \\ &\frac{a^4 (a^2 - \eta^2 s_1^2 (c_1 c_2 \eta + a s_2))^2 (a^2 - \eta^2 s_1^2 c_2^2)}{c_2 (\eta^2 s_1^2 (3c_2^2 + (c_1 c_2 \eta + a s_2)(c_1 c_2 \eta + 3a s_2)) + a^2 (5 + 3c_1^2 \eta^2))^{7/2}}, \end{aligned} \quad (49)$$

where

$$\eta = \sqrt{1-\tau^2}, \quad s_1 = \sqrt{1-c_1^2}, \quad c_2 = \sqrt{1-s_2^2}, \quad a = \sqrt{1-\eta^2 c_1^2}. \quad (50)$$

As in (34) and Figure 7, negative values of s_2 appear as they replace values of ϕ between $\pi/2$ and $3\pi/2$.

REFERENCES

- Acton, F. S. 1970, Numerical Methods that Work (Harper & Row)
- Atiyah, M., & Sutcliffe, P. 2002, Proc. Roy. Soc. Lond., A458, 1089, hep-th/0105179
- Backus, G. 1970, Rev. Geophys. Space Phys., 8, 633
- Bacry, H. 1974, J. Math. Phys., 15, 1686
- Battye, R. A. 1999, prepared for 2nd International Conference Physics Beyond the Standard Model: Beyond the Desert 99: Accelerator, Nonaccelerator and Space Approaches, Ringberg Castle, Tegernsee, Germany, 6-12 Jun 1999
- Bielewicz P., Eriksen H.K., Banday A.J., Gorski K.M., Lilje P.B., 2005, Astrophys.J., 635, 750, astro-ph/0507186
- Bogomolny, E., Bohigas, O., & Leboeuf, P. 1996, J. Stat. Phys., 85, 639, chaos-dyn/9604001
- Copi, C. J., Huterer, D., Schwarz, D. J., & Starkman, G. D. 2006, Mon. Not. Roy. Astron. Soc., 367, 79, astro-ph/0508047
- . 2007, Phys. Rev. D, 75, 023507, astro-ph/0605135
- Copi, C. J., Huterer, D., & Starkman, G. D. 2004, Phys. Rev. D, 70, 043515, astro-ph/0310511
- Courant, R., & Hilbert, D. 1953, Methods of Mathematical Physics, Vol. 1 (New York: Interscience Publishers)
- de Oliveira-Costa, A., Tegmark, M., Zaldarriaga, M., & Hamilton, A. 2004, Phys. Rev. D, 69, 063516, astro-ph/0307282
- Dennis, M. R. 2004, J. Phys. A, 37, 9487, math-ph/0408046
- . 2005, J. Phys. A, 38, 1653, math-ph/0410004
- Donoghue, E. P., & Donoghue, J. F. 2005, Phys. Rev. D, 71, 043002, astro-ph/0411237

- Efstathiou, G. 2004, *Mon. Not. Roy. Astron. Soc.*, 348, 885, astro-ph/0310207
- Eriksen, H. K., Banday, A. J., Gorski, K. M., Hansen, F. K., & Lilje, P. B. 2007, astro-ph/0701089
- Eriksen, H. K., Banday, A. J., Gorski, K. M., & Lilje, P. B. 2005, *Astrophys. J.*, 622, 58, astro-ph/0407271
- Eriksen, H. K., Hansen, F. K., Banday, A. J., Gorski, K. M., & Lilje, P. B. 2004a, *Astrophys. J.*, 605, 14, astro-ph/0307507
- Eriksen, H. K., Novikov, D. I., Lilje, P. B., Banday, A. J., & Gorski, K. M. 2004b, *Astrophys. J.*, 612, 64, astro-ph/0401276
- Gruppuso, A., Burigana, C., & Finelli, F. 2007, *Mon. Not. Roy. Astron. Soc.*, 376, 907, astro-ph/0701295
- Hannay, J. 1996, *J. Phys. A*, 29, L101
- Hansen, F. K., Balbi, A., Banday, A. J., & Gorski, K. M. 2004a, *Mon. Not. Roy. Astron. Soc.*, 354, 905, astro-ph/0406232
- Hansen, F. K., Banday, A. J., & Gorski, K. M. 2004b, *Mon. Not. Roy. Astron. Soc.*, 354, 641, astro-ph/0404206
- Hansen, F. K., Cabella, P., Marinucci, D., & Vittorio, N. 2004c, *Astrophys. J.*, 607, L67, astro-ph/0402396
- Haugboelle, T., et al. 2006, astro-ph/0612137
- Helling, R. C., Schupp, P., & Tesileanu, T. 2006, *Phys. Rev. D*, 74, 063004, astro-ph/0605594
- Hinshaw, G., et al. 2007, *Astrophys. J. Suppl.*, 170, 288, astro-ph/0603451
- Hobson, E. W. 1931, *The Theory of Spherical and Ellipsoidal Harmonics* (Cambridge University Press)
- Katz, G., & Weeks, J. 2004, *Phys. Rev. D*, 70, 063527, astro-ph/0405631
- Lachieze-Rey, M. 2004, astro-ph/0409081
- Land, K., & Magueijo, J. 2005a, *Phys. Rev. Lett.*, 95, 071301, astro-ph/0502237
- . 2005b, *Mon. Not. Roy. Astron. Soc.*, 357, 994, astro-ph/0405519
- . 2005c, *Mon. Not. Roy. Astron. Soc.*, 362, L16, astro-ph/0407081
- . 2005d, *Mon. Not. Roy. Astron. Soc.*, 362, 838, astro-ph/0502574
- . 2007, *Mon. Not. Roy. Astron. Soc.*, 378, 153, astro-ph/0611518
- Maxwell, J. C. 1891, *A Treatise on Electricity and Magnetism* (Clarendon Press)
- Mezei, M., & Campbell, E. S. 1976, *J. Comp. Phys.*, 20, 110
- Naselsky, P. D., Verkhodanov, O.V., Nielsen, M.T. B., arXiv:0707.1484
- Park, C.-G., Park C., Gott J.R., *Astrophys. J.*, 660, 959, astro-ph/0608129
- Park, C.-G. 2004, *Mon. Not. Roy. Astron. Soc.*, 349, 313, astro-ph/0307469
- Penrose, R., & Rindler, W. 1984, *Spinors and space-time, volume 1: Two-spinor calculus and relativistic fields* (Cambridge University Press)
- Prosen, T. 1996, *J. Phys. A*, 29, 4417
- Rakic, A., & Schwarz, D. J. 2007, *Phys. Rev. D*, 75, 103002, astro-ph/0703266
- Ralston, J. P., & Jain, P. 2004, *Int. J. Mod. Phys.*, D13, 1857, astro-ph/0311430
- Rigopoulos, G. I., Shellard, E. P. S., & van Tent, B. J. W. 2006, *Phys. Rev. D*, 73, 083522, astro-ph/0506704
- Schupp, P. 1999, *Comm. Math. Phys.*, 207, 481, math-ph/9902017
- Schwarz, D. J., Starkman, G. D., Huterer, D., & Copi, C. J. 2004, *Phys. Rev. Lett.*, 93, 221301, astro-ph/0403353
- Spergel, D. N., et al. 2003, *Astrophys. J. Suppl.*, 148, 175, astro-ph/0302209
- . 2007, *Astrophys. J. Suppl.*, 170, 377, astro-ph/0603449
- Tegmark, M., de Oliveira-Costa, A., & Hamilton, A. 2003, *Phys. Rev. D*, 68, 123523, astro-ph/0302496
- Vielva, P., Martinez-Gonzalez, E., Barreiro, R. B., Sanz, J. L., & Cayon, L. 2004, *Astrophys. J.*, 609, 22, astro-ph/0310273
- Wands, D. 2007, astro-ph/0702187
- Weeks, J. R. 2004, astro-ph/0412231
- Zou, W.-N., & Zheng, Q.-S. 2003, *Proc. R. Soc. A*, 459, 527

This paper has been typeset from a $\text{\TeX}/\text{\LaTeX}$ file prepared by the author.